# CHAOS THEORY and sEMG

G. Filligoi

*Abstract*— **The possibility of making inferences on motor unit (MU) recruitment and MU firing rate modulation from the analysis of the myoelectric signal recorded non-invasively from the skin surface has been variously addressed in the literature, sometimes with controversial results. As a matter of fact, it has been widely confirmed that some time- or frequency-domain parameters extracted from the surface ElectroMyoGram (sEMG) are strongly related to some fundamental mechanisms of motor control. The Root Mean Square (RMS) or the MeDian power spectral Frequency (MDF) are just two of them. In the last decade, improvement of recording techniques allowed a better and reliable estimate of the average muscle fiber Conduction Velocity (CV) from sEMG. Furthermore, the refinement of non-linear analysis technique (according to chaos theory) provided a further investigation instrument (commonly referred as the percentage of determinism, %DET) able to detect the presence of repetitive hidden patterns in sEMG which, in turn, senses the level of MU synchronization within the muscle. Moreover, new non-linear parameters (such as Lyapunov exponents, correlation dimension, fractal dimension, and so on) are under investigation for their ability to sense new particular aspects of neuromuscular mechanisms of movement control. In particular, in this paper some results on Lyapunov coefficients are reported.**

*Index Terms*— **surface EMG, neuromuscular control, chaos theory, percentage of determinism, Lyapunov exponents**

## I. Introduction

Biomedical signals carrying information about the physiological activities of human and animal organisms embrace several areas of interest, ranging from gene and protein sequences [1], to neural and cardiac rhythms [2], to neuromuscular control [3], to tissue and organ images [4], to sensory perception, control and coordination [6]. Biomedical signal processing aims at extracting significant information from biomedical signals. From the historical and conceptual point of view, the most important phases, which represent the main application of signal processing procedures to the investigation of living cells, organs, tissues, system, populations, are the direct consequences of the parallel computer SW/HW development. It has been possible to implement progressively sophisticated algorithms on more and more complicated machine structure in shorter execution times. In the next three sections, some of the mathematical concepts concerning biomedical signal processing evolution will be briefly examined.

Manuscript received 10 January 2011

G. Filligoi is with Dept of Information, Electronics and Telecommunication Engineering (DIET), Fac. Inform. Engineering, University La Sapienza, Via Eudossiana, 18 Roma 00184 (Italy)
2)-CISB (Center for Biomedical Engineering), Palazzo Baleani, University La Sapienza, Corso V. Emanuele II, 194 Roma 00192 (Italy) (corresponding author phone (+39)06.4458.5478; FAX: (+39)06.4873300; E-mail: giancarlo.filligoi@uniroma1.it).

## II. Time- and Frequency-domain analysis

This typical approach, widely used in electronic & telecommunication engineering, is based on the common (approximate) hypothesis that signals are generated by linear and time-invariant systems, for which the superposition principle is valid. Mathematically, for a linear system $F$, defined by $F(in) = out$, where $in$ is some sort of stimulus and $out$ is some sort of response, the superposition of several stimuli yields a superposition of the respective responses:

$$F(in_1+in_2+...+in_Q) = F(in_1) + F(in_2)+...+F(in_Q) \quad (1)$$

Moreover, the system permanency asks that a time-translation $\tau$ at the input provokes an analogous translation $\tau$ at the output:

$$\text{If } in(t) \rightarrow out(t) \text{ THEN } in(t+\tau) \rightarrow out(t+\tau), \forall\tau \quad (2)$$

For systems satisfying eq. (1) and (2), the Fourier Transform and the corresponding issues concerning the spectral estimate through periodograms, correlograms, ARMA models, Burg-algorithm, MUSIC or Pisarenko or De Prony approaches, are directly applicable. Decades ago, the primary focus of biomedical signal processing was on filtering signals to remove noise arising from imprecision of instruments and/or interference of power lines, or simply due to the biological systems themselves under study.

A fundamental method for noise cancellation analyzes the signal spectra and then suppresses undesired frequency components. Within this context, if the biomedical signal is represented by a mono-dimensional finite-length real vector $\boldsymbol{x(t)}$, the corresponding spectral content is given by the frequency-domain complex vector $\boldsymbol{X(f)}$:

$$\boldsymbol{x}(t),\ t\in[0,T] \ \underset{\leftarrow F^{-1}\{.\}}{\overset{F\{.\}\rightarrow}{<\text{---------}>}}\ \boldsymbol{X}(f),\ f\in(-\infty,+\infty); \quad (3)$$

$$\boldsymbol{with}\ \boldsymbol{X}(f)=Re[\boldsymbol{X}(f)] + j\ Im[\boldsymbol{X}(f)]$$

In this notation: $t$ denotes the time variable and $f$ the frequency dominium of the spectrum; $F\{.\}$ is the Fourier algorithm applied from left to right side of notation (3), and, viceversa, $F^{-1}\{.\}$ represents the opposite inverse operation from

frequency- to time-domain. The application of the Fourier operator $F\{.\}$ corresponds to carrying out the inner product between the signal and a function $\varphi(t)$ representing the complex exponential $exp(-j2\pi ft)$, $t \in (-\infty, +\infty)$:

$$X(f) = F\{x(t)\} \equiv < x(t),\ \varphi(t) > = \int [x(t) * exp(-j2\pi ft)]\, dt \qquad (4)$$

where the integral is extended to the interval $(-\infty, +\infty)$ by assuming that ouside the interval [0,T] of definition of the signal $x(t)$, the signal is identically null. The main advantage of the frequency- over the time-representation is that it allows a clear visualization of the frequency content of the signal variance and the enhancement of the periodicities of the signal, thus helping, in many cases, to understand underlying physical phenomena. On the contrary, there are two main disadvantages: a)- Most bio-signals are generated by intrinsically non-stationary sources, hence frequency approach can be used only in an interval of (approximate) stationarity; b)- Since the Fourier Transform is based on comparing the signal with complex sinusoids that extend through the whole time domain, the information about the time evolution of the frequencies is completely lost.

## III. Time-Frequency Distribution & Wavelet Transform

For all occasions in which signals have time varying features that cannot be resolved with the Fourier Transform, the problem is partially resolved by using the Gabor Transform $\mathcal{G}_w(f,t)$ [8], also called Short-Time Fourier Transform (STFT):

$$\mathcal{G}_w(f,t) \equiv < x(t),\ w_T(t'-t)\, exp(-j2\pi ft') > \qquad (5)$$

With this approach, the evolution of the frequencies can be followed and the stationarity requirement is partially satisfied by considering the signals to be stationary in the order of the window length. A wider class of (f,t) distributions can be obtained (the so-called *Generalized Cohen Class t-f distributions,* [7]) by substituting $w_T(t)$ with more generalized kernels $\xi(t)$ whose aim is to increase the local convergence of the inner product by means of decaying functions.

On the other hand, though Gabor Transform gives an optimal time-frequency representation, one intrinsic critical limitation on data windowing derives from the Uncertainty Principle: if the window is too narrow, the frequency resolution will be poor, and if the window is too wide, the time localization will not be very precise. Data involving slow processes will require wide windows and on the other hand, for data with fast transients (high frequency components) a narrow window will be more suitable. Then, due to its fixed window size, Gabor Transform is not suitable for analyzing signals involving different range of frequencies in different time-windows. To overcome this problem, the Wavelet Transform (WT) was introduced in 1984 [9]. The main advantage of wavelets is that they have a varying window size, being wide for slow frequencies and narrow for the fast ones, thus leading to an optimal time-frequency resolution in all the frequency ranges (Fig.1). Furthermore, due to the fact that windows are adapted to the transients of each scale, wavelets lack of the requirement of stationarity. Mathematically, WT is the result of the inner product between the signal and a wavelet family $\psi_{a;b}(t)$. The former set of elemental functions is generated by dilations $b$ and translations ($a$ scale parameter, $a \neq 0$) of an admissible mother wavelet $\psi(t)$:

$$\psi_{a;b}(t) = |a|^{-1/2}\ \psi[(t-a)/b] \qquad (6)$$

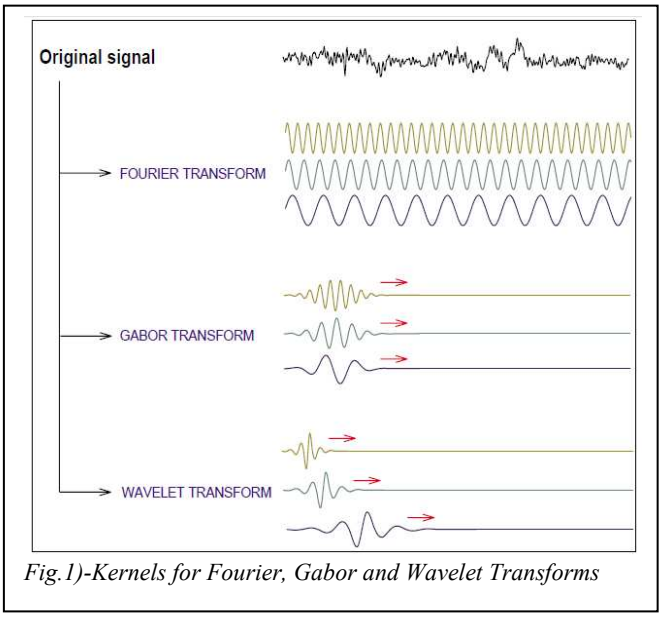


*Fig.1)-Kernels for Fourier, Gabor and Wavelet Transforms*

As the parameter $a$ increases the wavelet becomes narrower and by varying $b$ the mother wavelet is displaced in time. The continuous wavelet transform of a signal $W_{\psi,x}(a,b)$ is given by:

$$W_{\psi,x}(a,b) = < x(t),\ \psi_{a;b}(t) > \qquad (7)$$

thus providing a time-scale representations of the $x(t)$ signal content. The correlations in (7) indicate precisely how the wavelet function locally fits the signal at every scale $a$.

## IV. Chaos Theory

Chaotic approach to system & signal analysis falls within the dynamic non-linear system studies. Accordingly, biomedical signals can be to an extent deterministic, random or chaotic: a)-deterministic signals have the characteristic of predictability, meaning that any future course of the signal could be predicted using some linear analysis tools. For them, mathematical tools (e.g., Fourier transform) are commonly used; b)-random signals are non-deterministic in the sense that individual data points of the signal may occur in any order, with no predictability on the future course of the signal (stochastic processes). Only purely stochastic analytic tools can be applied; c)-chaotic signals can be viewed as a connecting mesh between deterministic and random signals, exhibiting behaviour that is slightly predictable, non-periodic or seldom quasi-periodic (e.g., heart beat), and highly sensitive to initial conditions.

Within chaos theory, the system which generates the chaotic signals will be represented in the phase-space. It can be inferred that the observed signal vector ***x(n)*** is a projection of the signal generator source, represented by an unknown, but underlying multidimensional dynamic state vector. The state vector is composed of an unknown number of variables, represented through its dimension, called Embedded Dimension *ED*. The transition from a sampled one-dimensional time-domain signal ***x(n)*** to the corresponding sampled *ED*-dimensional state space requires the application of Takens Theorem [10]. With this technique, we can reconstruct an approximation ***s(i)***, $i \in [1,..,m]$ in *ED*-dimensional state space of the unknown dynamic state vector by lagging and embedding the observed time-series ***x(n)***. This reconstructed approximation is the set ***S(m)*** of all state vectors ***s(i)*** in the phase space:

$$\mathbf{S}(m) = [\mathbf{s}(1), \mathbf{s}(2), \ldots, \mathbf{s}(m)] \ , \ m = n - \lambda\,(ED-1) \qquad (8)$$

each of them composed of *ED* time-delayed samples of ***x(n)*** , where $\lambda$ represents the time-delay:

$$\mathbf{s}(i) = [\,\mathbf{x}(i)\ \ \mathbf{x}(i+\lambda)\ \ \ldots\ \mathbf{x}(i+\lambda(ED-1))], \ i=1,..m \qquad (9)$$

The accurate estimation of ED and λ guarantees through the Embedding Theorem [5, 14, 17] that the sequential order of the reconstructed state vector ***s(i)→s(i+1)*** is topologically equivalent to the transition of signal vector generator ***x(i)→x(i+1)***. Each state space coordinate ***s(i)*** constituting a component of ***S(m)*** defines a point in the state space. As time progresses, the dynamic trajectory of each point in time forms the so-called *orbit* or *trajectory*. An orbit is mathematically defined as the numerical trajectory resulting from the solution of the autonomous set of differential equations which govern the system responsible for the generation of ***x(n)***.

The order of the set of differential equations is strictly related to *ED*, which, in a way, represents its approximation: therefore, the more complex is the represented system, the higher is that order, and hence *ED*. The time delay λ is an integer multiple of the sampling interval of the signal ***x(n)*** guaranteeing the extraction of maximal amount of information from the system, so that the time-delayed space coordinates forming ***S(m)*** are independent from each other. The independence between two coordinates of the time-delayed state space can be assessed either using the first zero of the sequence autocorrelation (which guarantees that for that lag $j_0$ the samples are statistically independent) or the first minimum of the mutual information between two ***s(i)*** coordinates (e.g., ***x(i)*** and ***x(i+λ)*** ). The former asks for the assessment of the discrete autocorrelation $R_{xx}(j)$ at each lag $j$ for the discrete real signal ***x(n)***:

$$\lambda = j_0 : \xrightarrow[1st-ZERO]{} R_{xx}(j) = E[x_n x_{n-j}] \equiv \lim_{n\to\infty} \frac{1}{N} \sum_{n=0}^{N-1} x_n x_{n-j} \qquad (10)$$

where *E[.]* means *expected value*. For finite time-width signals ***x(n)***, $n \in [0,N-1]$ (hypothesis always valid for recorded biomedical signals) the autocorrelation can be equally estimated by the biased or unbiased estimators respectively given by:

$$R_{xx}(j) = \frac{1}{N} \sum_{n=0}^{N-1} x_n x_{n-j} \qquad (11a)$$

$$R_{xx}(j) = \frac{1}{N-j} \sum_{n=0}^{N-1} x_n x_{n-j} \qquad (11b)$$

Alternatively, the independence of two ***s(i)*** coordinates (e.g., ***x(i)*** and ***x(i+dλ)***, $\forall\, d \in [1,ED]$) can be assessed using also the mutual information (*MI*) function. For instance, the *MI* (for *d=1*) is measured in bits by:

$$MI = \log_2 \left\{ \frac{P[x(i), x(i+\lambda)]}{P[x(i)]P[x(i+\lambda)]} \right\} \qquad (12)$$

where ***P[x(i),x(i+λ)]*** is the joint probability density function (*JPDF*) of ***x(i)***, and ***x(i+λ)***. The average mutual information (*AMI*) of the *JPDF* of all coordinates is calculated by:

$$\lambda : \xrightarrow[1st-MIN]{} AMI(\lambda), with$$

$$AMI(\lambda) = \sum_{[x(i),x(i+d\lambda)],\forall d} P[x(i), x(i+\lambda)] \log_2 \left\{ \frac{P[x(i), x(i+\lambda)]}{P[x(i)]P[x(i+\lambda)]} \right\} \qquad (13)$$

The first minimum of the AMI function provides the optimal value for the time-delay $\lambda$, and assures the independence between the coordinates of the multi-dimensional vector ***s(i)***.

Concerning *ED* evaluation, the signal reconstruction in state space requires a dimension that will guarantee no overlap of the trajectory of the orbit constituting the phase space. This optimal dimension is obtained after calculating the percentage of False Nearest Neighbours (*FNN*) between points in state space, while FNN are evaluated using reconstructed state space vectors ***S(m)*** at different *ED*, but at constant λ [5, 11÷14]. It is accepted that when the *FNN* percentage drops to zero, the minimum required dimension to unfold the system into its original state around its attractor is reached, which also guarantees that the orbit is unique. The *FNN* calculation requires the measurement of the distance between neighbor vectors in consecutive *ED* dimensions. Determining the existence of *FNN* depends on how such distance behaves as the calculations progress while *ED* increases. Referring to Fig. 2, we may observe that for chaotic systems *FNN* presents an evident knee behavior for certain values of *ED* (e.g., for the chaotic signal in Fig.2 about *ED* ≅ 12÷15): when FNN increases significantly with the ED increment, then the vectors are false neighbors, and their closeness results from the

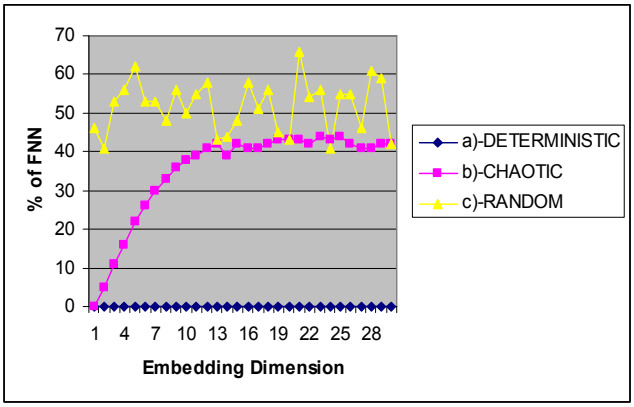


*Fig.2)-Sample dynamics of t% FNN as a function of the ED for deterministic (a), chaotic (b), and random (c) signals.*

reconstruction dynamics of the system, not from its underlying dynamics. If the distance is restricted within a certain threshold level close to the state space points, then the state space points are real neighbors resulting from the dynamics of the system. The embedding dimension that adequately represents the system is the dimension that eliminates most of the false neighbors, leaving a system whose trajectories are positioned in state space due to their underlying dynamics, not to their reconstruction dynamics [12-14].

## V. Chaotic approach to biomedical signals

Based on the previous general chaotic-theory approach to be applied to several scientific fields, advances in computer technology allowed studying the behavior of non linear systems of differential equations, for which there are solutions very difficult to find in a close mathematical form (or, often, no solutions at all) [15, 17]. In these cases, the approximate discrete solutions are the only ones available.

Within biomedical signal processing, chaotic dynamics provide a possible explanation for the different complex and erratic patterns that appear in most bio-signals [16]. In general, the range of applications of non-linear techniques applied to problems in biomedicine is rapidly expanding and spans from studies of brain rhythms [22-25], to heart beat [18-21], from blood pressure regulation [37, 38] to neuromuscular system [14, 26-36], from breathing system [39] to cardio-respiratory coordination [40], from genomic & proteomic sequences (e.g., DNA and RNA, proteins) [40, 43] to complexity of the human and animal anatomo-physiological systems [41, 42].

At this point, an obvious question arises: starting from the phase-space representation of the chaotic system responsible for the generation of the observed signal, how to represent its behaviour? Or, better, which parameters better represent a non-linear dynamic system? An exhaustive response to this question is beyond the scopes of this paper devoted to the application of chaos theory to sEMG (surface EMG).

## VI. Non-linear analysis of sEMG

The sEMG signal is a highly non-stationary signal, especially when the limb or the body segment under interest is rapidly moving. In fact, in these cases the neuromuscular control process works through facilitating or inhibiting feed-back mechanisms implemented on neuronal circuitry involving the Central Nervous System at various cortical or sub-cortical levels. Besides, these considerations further encourage the adoption of non-linear analysis techniques for taking into account for the highly non-linear behavior of such mechanisms using muscle receptors (muscle spindle and Golgi Tendon Organs which are interlaced in parallel or in series with the muscle fibers within the muscle), mechanoreceptors (Pacinian corpuscles, Meissner's corpuscles, Merkel's disks, Ruffini corpuscles), nociceptors, and joint receptors within local (spinal) and/or central sensory-motor networks. In our opinion, non-linear parameters reveal several hidden mechanisms of muscle control that otherwise would be not reflected by variability of other "classic" linear parameters, such as RMS (Root Mean Square), AVR (Averaged Rectified Value), Mean (MNF) and Median frequency (MDF).

In our concern, two main non-linear parameters are described:

a)-**Percentage of determinism (%DET).**

Relative Recurrence Quantification Analysis (RQA) is a non-linear sEMG analysis firstly introduced by Webber et al. [44] and Nieminen and Takala [45]. RQA, described by Eckmann et al. [46], is based on a graphical method originally designed to locate recurring patterns (hidden rhythms) and non-stationarities (drifts) in experimental data sets. With RQA technique, the sEMG signal $\boldsymbol{x(i)}$ is mapped in a bi-dimensional space (the *recurrence map*), thus makings possible to identify time-recurrences that are not readily apparent in the original recordings, either by qualitative visual inspection or by evaluating some specific variables. This method has been recently used in some experimental surface EMG studies [32÷36] which showed its potential in detecting changes of muscle properties due to fatigue. Referring to Fig. 3, after the Embedding Procedure which projects the signal $\boldsymbol{x(i)}$ onto the phase-space, a *Distance Matrix,* which represents the closeness of all possible state vectors pairs:

$$\boldsymbol{s(i)}, \boldsymbol{s(j)}, \ \forall i, \ \forall j, \ i.,j=1,..m; \ m= n - \lambda \ (ED-1) \tag{14}$$

is introduced. For this purpose, the Euclidean distance between them is evaluated:

$$d(i,j) = [ < (\boldsymbol{s(i)}, \boldsymbol{s(j)})^2 > ]^{1/2} \tag{15}$$

In order to make the distance evaluation independent of the energy of the observed signal, the usual effective values adopted in RQA are either expressed as a percentage of the maximal distance (considered as 100) or normalized with respect to the average distance between vectors:

$$d_{av} = \frac{\sum_{i=1}^{m}\sum_{i\neq j}^{m} d(i,j)}{m.(m-1)/2} \tag{16}$$

where the denominator represents the number of distances $d(i,j)$. A *recurrence plot rp* is finally obtained as a map of pixels which assume the values '0' or '1' on the basis of a threshold set on the *Distance Matrix*.

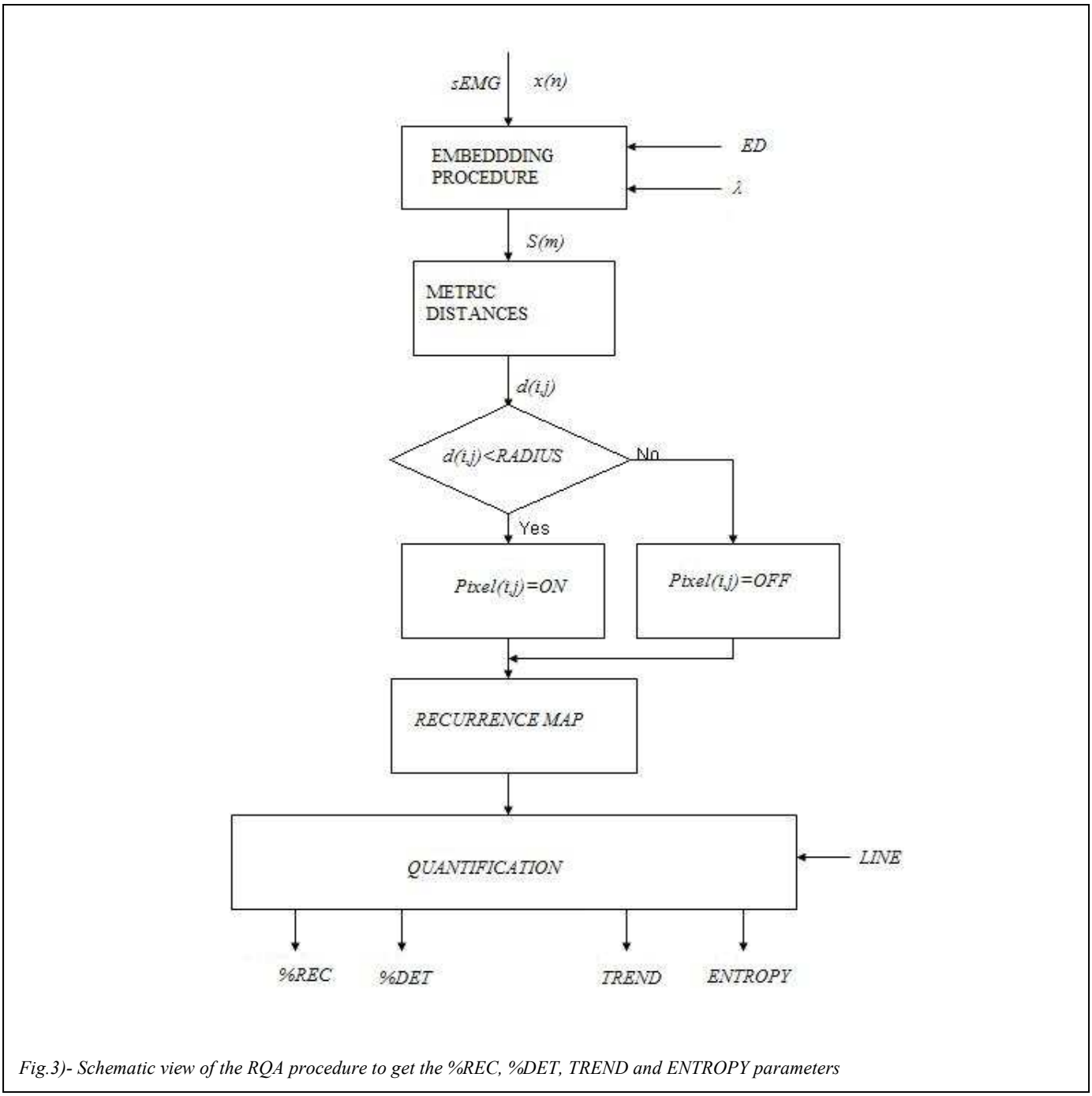


*Fig.3)- Schematic view of the RQA procedure to get the %REC, %DET, TREND and ENTROPY parameters*

For this purpose, the following comparison between states is accomplished:

$$\text{IF } d(i,j) \leq \text{threshold THEN } rp(i,j) = \text{ON} \quad \text{ELSE } rp(i,j) = \text{OFF} \tag{17}$$

and provides the *Recurrence Map* as the collection of all $rp(i,j)$, $\forall\ i,j$.

A representation of all possible recurrence plots (with 1 sec epoch lengths), during a 18 sec isometric contraction, is given in fig.4. The threshold operation in eq. (17) is conceptually equivalent to considering two states of the dynamical system as close to each other when the embedded vectors $\mathbf{s}(i)$ and $\mathbf{s}(j)$ are enclosed in an *ED*-dimensional hyper-sphere with radius equal to the selected threshold. Fine tuning of the threshold value has to be carried out for all sets of sEMG data recorded within an experimental protocol since it is strictly related to the variables extracted from the procedure of quantifying the *Recurrence Map***.** Figure 5 (to be described below in more details) shows an example of recurrence maps of synthetic signals. Since *recurrence maps* contain subtle patterns that are often difficult to detect by visual inspection, some quantitative descriptors that emphasize different features of the map have been introduced (in Fig. 3 four mostly used parameters *%REC, %REC, TREND*, and *ENTROPY*, are considered) [47]. Among them, percentage of determinism (*%DET*) has been widely used by our research group and describe the percentage of points that form upward diagonal lines (with length greater than a prefixed cut-off value *LINE*)

*Fig.4)-Collection of 18 sEMG recurrence plots*

with respect to the number of pixels ON in the *Recurrence Map*. In particular, we have shown, either based on real sEMG or simulated data, that *%DET* is strictly connected to the level of MU synchronization. Referring to Fig. 5, sEMG simulated signals generated by a model [48] at 0% or 25% MU synchronization level shows an evident increase of the *%DET* parameter while passing from lower (a) to higher (b) levels of MU synchronization [33]. Analogously, we may expect that a similar strategy will be used by the neuromuscular control system when the muscle task asks for the maintenance of the effort for a long period of time. Surely, a greater synchronization of the MU activation will help to satisfy this request, despite the contemporaneously increased fatigue. As a matter of fact, this hypothesis is confirmed by the sEMG recorded in weight-lifters during a 20 second maximal isometric contraction [32]. In Fig. 6, the sEMG recorded from vastus lateralis muscle during the first

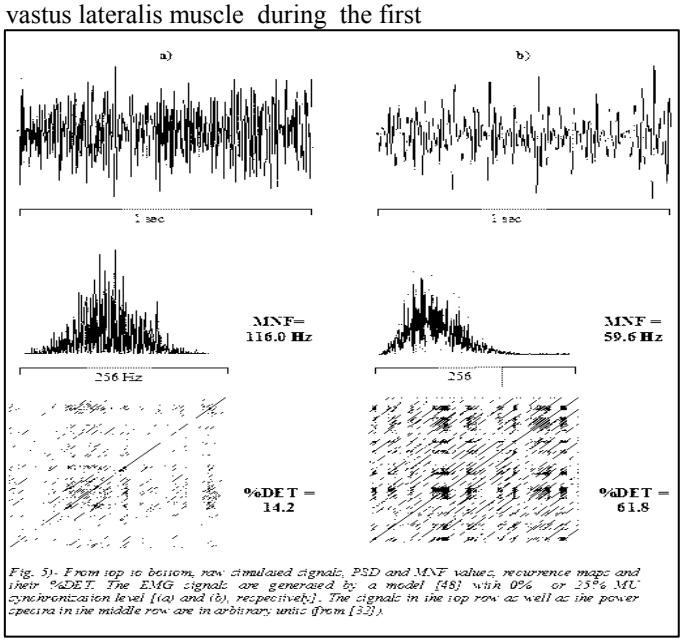


*Fig. 5)- From top to bottom, raw simulated signals, PSD and MNF values, recurrence maps and their %DET. The EMG signals are generated by a model [48] with 0% or 25% MU synchronization level (a) and (b), respectively. The signals in the top row as well as the power spectra in the middle row are in arbitrary units (from [33]).*

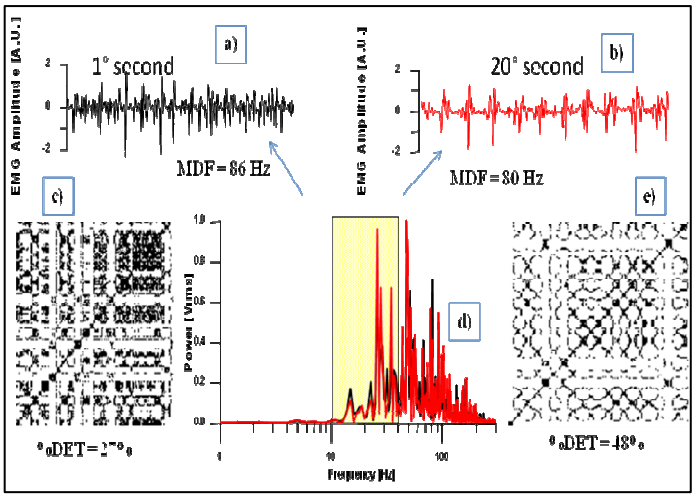


*Fig.6)- Real sEMG recorded in weight-lifters at the beginning (a) and at the end (20 seconds) (b) of a maximal effort at 100% MVC: the corresponding power spectra are shown at the center of the figure (d) together with the relative recurrence plots (1st second in c and 20th second in e). The corresponding values of MDF and %DET are also given.[from 32]*

and the last second of muscle task are reported. It is evident that, whereas very little differences in the relative spectra are reflected also in the MDF parameter weakly sensitive to the variation of the muscle status, increasing fatigue phenomena ask for a higher level of MU synchronization sensed by a parallel increase in the non-linear parameter %DET.

Analogously, if we refer to physiological findings widely accepted in the literature on the strategies used by the neuromuscular system for progressively muscle strength increasing [3], we may expect that during an increasing ramp the relative timing of the phenomena are:

- i)-at the beginning of the force ramp, there is an increasing level of MU recruitment followed by firing rate increase of the active MU;
- ii)-MU derecruitment will start as soon as the rapid and little MU firstly recruited become fatigued;
- iii)-the equilibrium between recruitment of the slower & bigger MUs and MU derecruitment determines the phase called MMUR (Maximal Motor Units Recruitment) in the figure which corresponds to the highest level of MU active in that muscle;
- iv)-after that phase, an increase in muscle strength can be obtained either by firing rate increase or MU synchronization increase.

The ramp phase is also characterized by a variation of the average muscle fibre Conduction Velocity (CV) along the course of the whole task. In general, the relative timing influencing the characteristics of the sEMG during a 0÷100%MVC ramp depends either on experimental procedure (ramp slope, muscle investigated, etc.) or on subjective variables (motivation, level of training, anatomy & physiology of the neuromuscular system investigated, and so on). As a matter of fact, while the increase in firing rate operates along the whole force ramp [49], the role of MU

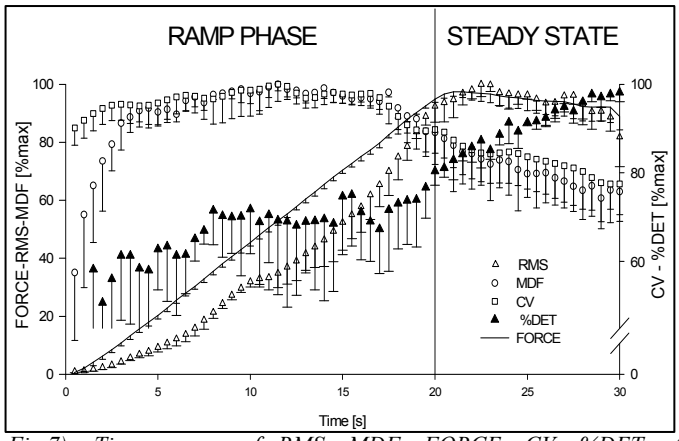


*Fig.7)- Time course of RMS, MDF, FORCE, CV, %DET at 5%MVCper sec. Data are averages (±SD) of all tests performed by all subjects and normalized to their maximum value (from [34, 35]).*

recruitment/derecruitment cannot be ascertained by needle EMG either.

Considering the results [34, 35] reported in fig. 7 obtained during a slowly varying force ramp (at *5% MVC /sec*, where *MVC=Maximal Voluntary Contraction*), we may observe that both linear and non-linear parameters can help understanding some of the control strategies employed by the neuromuscular system. In particular: a)-*MDF* increases up rapidly to a maximum due to corresponding increase of fast&little MUs early recruited , presumably corresponding to a Maximum MU Recruitment (M.M.U.R.) point [49, 50]; b)-the *CV* increases till the end of the ramp phase, since the faster MUs are last recruited, according to the "size principle" of Hennemann; c)-*%DET*, after a rapid increase, flattens for a long interval at the middle of the ramp, as a result of the equilibrium between the effects of CV increase (that would decrease %DET [33, 34]) and those of increasing MU synchronization, that would tend to increase the parameter; d)-RMS increases with the force with an exponential fashion. In all our experiments, this exponential growth is suddenly interrupted around a flex point and then continues. In the next sub-section, we will examine another non-linear parameter.

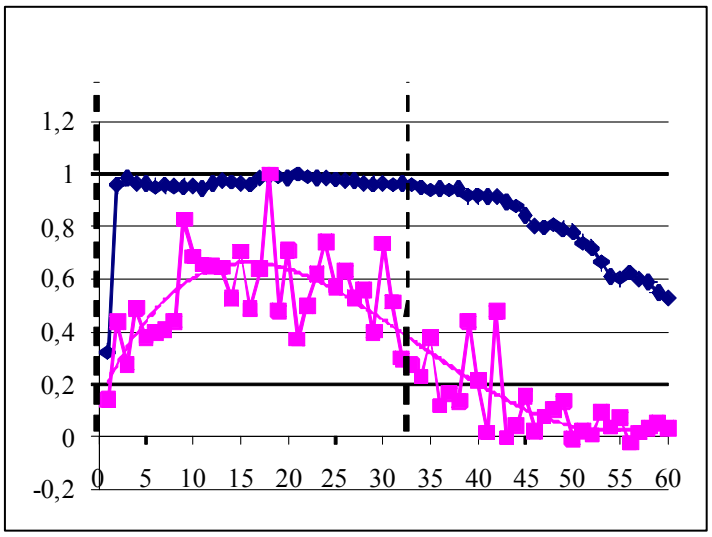

**b)-Lyapunov exponent** of a dynamical system is a quantity that characterizes the rate of separation of infinitesimally close trajectories. Quantitatively, two trajectories in phase-space, with initial separation $\Delta Z_0$, diverge as:

$$\left|\Delta Z(t)\right| \approx e^{\lambda t}\left|\Delta Z_0\right| \tag{18}$$

where λ is the Lyapunov exponent.

The rate of separation can be different for different orientations of initial separation vector. Thus, there is a spectrum of Lyapunov exponents, equal in number to the dimensionality ED of the *phase space*. The whole set of Lyapunov exponents provide:

- a measure of system chaoticity, e.g., system sensitivity to initial condition variations;

*Fig.8)-Force(◊) and $L_1$ Lyapunov exponent (□) during MVC*

- a convergence/divergence measure between trajectories, each of them obtained by joining the points of phase-space occupied by the system along its time evolution.

The maximal Lyapunov exponent $L_1$ can be defined as follows:

$$L_1 \equiv \lambda = \lim_{t\to 0}\lim_{\Delta Z_0 \to 0}\frac{1}{t}\ln\frac{\left|\Delta Z(t)\right|}{\left|\Delta Z_0\right|} \tag{19}$$

In a way, the $L_1$ exponent supplies a notion of predictability for the dynamical system: a positive value is usually taken as an indication that the system is chaotic (provided some other conditions are met, e.g., phase space compactness). In fig.8, the time-course of the Lyapunov exponent L1 during an endurance test (i.e., a muscle task where the subject has to maintain its MVC for several repeated periods of time, 33 sec in the fig) is reported in squares (against the force, in rhombs).

As expected, chaoticity increases at the beginning of the muscle task, as the result of further MUs recruitment, and then decreases in presence of fatigue phenomena and MUs synchronization.

ACKNOWLEDGMENT

The English revision by Dr. Berenice Cocciolillo, english mother tongue, from the Gospel&Spiritual SoulSingers Chorus (www.soulsingers.it), is kindly acknowledged. .

REFERENCES

[1] I. Shmulevich, and E.R. Dougherty "Genomic Signal Processing (Princeton Series in Applied Mathematics)" *Princeton University Press*, July 2007.

[2] L. Särnmo, and P. Laguna "Bioelectrical signal processing in cardiac and neurological applications" *Elsevier (Amsterdam)*, 2005.

[3] R. Enoka "Neuromechanics of human movement" *Human Kinetics publ., Champaign (USA)*, 4th Ed., July 2008.

[4] A. Oppelt (Ed.) "Imaging systems for medical diagnostics" *Wiley-VCH, NY (USA)*, November 2005.

[5] H. D. I. Abarbanel "Analysis of observed chaotic data" *Springer, New York (USA)*, 1996.

[6] Team Bunraku (Ed) "Perception, decision and action of real and virtual humans in virtual environments and impact on real environments" *Activity Report of the Institute National de recherché en*

*informatique et en automatique, Rennes (France)*, 2009 (available at http://ralyx.inria.fr/2009/Raweb/bunraku/bunra ).

[7] L. Cohen "Time-frequency analysis" *Prentice-Hall, New Jersey (USA)*, 1995.

[8] S. Qian, and D. Chen "Joint time-frequency analysis: methods and applications" *Prentice Hall New Jersey (USA)*, 1996.

[9] A. Grossmann, and J. Morlet "Decomposition of Hardy Functions into square integrable wavelets of constant shape" *SIAM J. Math. Anal.*, vol. 15, pp. 723-736, 1984.

[10] F. Takens "Detecting strange attractors in turbulence" in: D.A. Rand, and L.S. Young (Eds) "Lecture notes in mathematics" *Springer, Berlin (Germany),* 1981, vol. 898, pp. 366-381.

[11] M.B. Kennel, R. Brown, and H.D.I Abarbanel "Determining embedding dimension for phase-space reconstruction using a geometrical reconstruction" *Physical Review A*, vol.45, pp. 3403-3411, 1992.

[12] C.N. Price, R. J. de Sobral Cintra, D.T. Westwick, and M. Mintchev "Classification of biomedical signals using the Dynamics of the False Nearest Neighbours (DFNN) algorithm" *Int. J. Inform. Theory & Applications*, vol. 12 (1), pp. 18-28, 2005.

[13] E.A. Clancy, D. Farina, G. Filligoi "Single channel techniques for information extraction from the surface EMG signal," in *Electromyography: Physiology, Engineering, and Non-Invasive Applications*, 1st ed., R. Merletti, P. Parker, Eds. N.Y. (USA) :Wiley-IEEE Press, pp. 281-305, July 2004.

[14] G. Filligoi, F. Felici, "Detection of hidden rhythms in surface EMG signals with a non-linear time-series tool" *Medical Engineering & Physics*, 1999, 21, 439-448.

[15] R. Bellman, "Methods of nonlinear analysis" *Academic Press (series in Mathematics in science and engineering), New York (USA)*, 1973.

[16] B. J. West, "Fractal physiology and chaos in medicine", *Word Scientific, Singapore,* 2000.

[17] S. Wiggins, "Introduction to applied non linear dynamical systems and chaos" *Springer, 2nd ed., Bristol (UK)*, 2000.

[18] A.R. Goldberger, J.W. Bruce, "Application of non linear dynamics to clinical cardiology" *Ann. Acad. Sci.,* pp. 195-212, 1985.

[19] D.T. Kaplan, R.J. Kohen, "Is fibrillation chaos?", *Circ. Res*., vol. 67, pp. 886-900, 1990.

[20] M. Richter, T. Schreiber, D.T. Kaplan, "Foetal ECG extraction with non-linear state space projections" *IEEE Trans. Biomed. Eng*., vol. 45, pp.133-137, 1998

[21] X.S. Zhang, Y.S. Zhu, Z.Z. Wang, N.V. Thakor "Detecting ventricular tachycardia and fibrillation by complexity measure" *IEEE Trans. Biomed. Eng.*, vol. 46, pp.548-555, 1999.

[22] I. Yaylali, H. Koçak, P. Yayakar "Detection of seizures from small samples using nonlinear dynamic system theory" *IEEE Trans. Biomed. Eng*., vol. 43, pp.743-751, 1996.

[23] A. Babloyantz, J.M. Slazar, "Evidence of chaos dynamic of brain activity during the sleep cycle" *Phys. Lett*., vol. 111 A, pp. 152-156, 1985.

[24] H. Adeli, S. Ghosh-Dastidar, N. Dadmehr "A Wavelet-Chaos Methodology for Analysis of EEGs and EEG Sub-bands to detect Seizure and Epilepsy", *IEEE Trans. Biomed. Eng.*, vol. 54 (2), pp. 205-211, 2007.

[25] H.Osterhage, F. Mormann, T. Wagner, K. Lehnertz, "Measuring the Directionality of Coupling: Phase Versus State Space Dynamics and Application to EEG Time Series," *International Journal of Neural Systems*, vol.17 (3), pp. 139-148, 2007.

[26] R.E. Kearney, J.W. Hunter, "Non linear identification of stretch reflex dynamics" *Ann. Biomed. Eng*., vol. 16, pp. 79-94, 1988.

[27] A.T. Moser, D. Graupe, "Identification of non-stationarity models with application to myoelectric signals for controlling electrical stimulation of paraplegics" *IEEE Trans. Acoustics Speech Signal Proc*., vol. ASSP-37, pp.713-719, 1989.

[28] M. Song, D.B. Segala, J.B. Dingwell, D. Chelidze "Slow-time changes in human EMG muscle fatigue states are fully represented in movement kinematics" *J. Biomech. Eng.,* vol. 131, feb 2009 (DOI: 10.1115/1.3005177).

[29] J. Dingwell, D.F. Napolitano, D. Chelidze "A non-linear approach to tracking slow-time scale changes in movement kinematics" *J. Biomech.*, vol. 40, pp. 1629-1634, 2007.

[30] P. Sbriccoli, F. Felici, A. Rosponi, A. Aliotta, V. Castellano, C. Mazzà, M. Bernardi, M. Marchetti, "Exercise induce muscle damage and recovery assessed by means of linear and non linear sEMG analysis and ultrasonography" *J. Electromyogr. Kinesiol.,* vol. 11, pp. 73-83, 2001.

[31] X. Hu, Z.Z. Wang, X.M. Ren "Classification of surface EMG signal with fractal dimension" *J. Zhejiang Univ SCI.*, vol. 6B (8), pp. 844-848, 2005.

[32] F. Felici, A. Rosponi, P. Sbriccoli, G. Filligoi, L. Fattorini, M. Marchetti "Linear and non-linear analysis of surface electromyograms in weightlifters" *Eur. J. Appl. Physiol*., vol. 84, pp. 337-342, 2001.

[33] D. Farina, L. Fattorini, F. Felici, and G. Filligoi "Non linear surface EMG analysis to detect changes of motor unit conduction velocity and synchronization" *J. Appl. Physiol*., vol. 93, pp. 1753-1763, 2002.

[34] G. Filligoi, F. Felici, P. Sbriccoli, L. Fattorini, I. Bazzucchi, A. Rosponi "Linear and non-linear EMG analysis improves knowledge of Neuromuscular Motor Control" *International Journal of Computer Science in Sport,* vol. 2, pp. 95-97, 2003.

[35] G. Filligoi "Parameters extracted from sEMG to infer motor control strategy" Proc. of the *III Internat. Congress on Computational Bioengineering*, pp. 307-312, 17-19 Sept. 2007, Isla de Margarita (Venezuela), ISBN: 978-980-6939-10-3.

[36] F. Felici, I. Bazzucchi, L. Fattorini, E. Ortuso, A. Bavetta, V. Paoluzzi, and G. Filligoi "Concentric-Eccentric force transients: linear and non-linear sEMG analysis," *Proc. XVIII Intern. Congr. ISEK (Intern. Society of Electrophysiol. and Kinesiology)*, Aalborg (Denmark), 16-19 June 2010, ISBN: 978-87-7094-047-4.

[37] Y. Almong, O. Oz, S, Akselrod "Correlation dimension estimation: can this non linear description contribute to the characterization of blood pressure control in rats?" *IEEE Trans. Biomed. Eng.,* vol. 46, pp.535-547, 1999.

[38] C.D. Wagner, P.B. Persson, "Non linear chaotic dynamics of arterial blood pressure and renal flow" *Amer. J. Physiol*.,*(Heart Circ. Physiol.),* vol. 268, n. 37, pp. H621-H627, 1996.

[39] M. Akay, E.J.H. Mulder "Effects of maternal alcohol intake on fractal properties in human fetal breathing dynamics" *IEEE Trans. Biomed. Eng.,* vol. 435, pp.1097-1103, 1998.

[40] D. Hoyer, R. Bauer, B, Walter, U. Zwiener "Estimation of non linear coupling on the basis of complexity and predictability – A new method applied to cardio-respiratory coordination" *IEEE Trans. Biomed. Eng.,* vol. 45, pp. 545 -552, 1998.

[41] F. Grizzi, M. Chiriva Internati "The complexity of anatomical systems" *Theoretical Biology and Medical Modelling*, vol. 2, 2005 [available at http://www.tbiomed.com/content/2/1/26 (doi:10.1186/1742-4682-2-26)]

[42] M. Bianciardi, P. Sirabella, G.E. Hagberg, A. Giuliani, J.P. Zbilut, A. Colosimo "Model-free analysis of brain fMRI data by recurrence quantification". *NeuroImage*, vol. 37 (2), pp. 489-503, 2007.

[43] A. Porrello, S. Soddu, J.P. Zbilut, M. Crescenzi, A. Giuliani "Discrimination of single amino acid mutations of the p53 protein by means of deterministic singularities of recurrence quantification analysis", *Proteins-structure function and bioinformatics,* vol 55, pp. 743-755, 2004.

[44] C.L. Webber, M.A. Schmidt, S.M. Walsh "Influence of isometric loading on biceps EMG dynamics as assessed by linear and non linear tools" *J. Appl. Physiol*., vol. 78, pp.814-822, 1995.

[45] H. Nieminen, E.P. Takala, "Evidence of deterministic chaos in the myoelectric signal" *Electromyogr. Clin. Neurophysiol*., vol. 36, pp. 49-58, 1996.

[46] J.P. Eckmann, S.O. Kamphorst, D. Ruelle "Recurrence plots of dynamical systems" *Europhys. Lett.,* vol. 4, 973-977, 1987.

[47] C.L. Webber, J.B. Zbilut, "Dynamical assessment of physiological systems and states using recurrence plot strategies" *J. Appl. Physiol*., vol. 76, pp. 965-973, 1994.

[48] D. Farina, R. Merletti "A novel approach for precise simulation of the EMG signal detected by surface electrodes" IEEE Trans. Biomed. Eng., vol. 48, pp. 637-645, 2001.

[49] M. Solomonow, C. Baten, J. Smith, R. Baratta, H. Hermens, R. D'Ambrosia, H. Shaoji "Electromyogram power spectra frequencies associated with motor unit recruitment strategies*" J. Appl. Physiol.*, vol. 68, pp. 1177-1185, 1990.

[50] P. Sbriccoli, I. Bazzucchi, A. Rosponi, M. Bernardi, G. De Vito, F. Felici "Amplitude and spectral characteristics of biceps brachii sEMG depend upon speed of isometric force generation" *J. Electromyogr. Kinesiol.*, vol. 13, pp. 139-147, 2003